

A Model for the $\text{Pr}_{1-x}\text{Ca}_x\text{MnO}_3$ Series with $x = 0.30-0.50$ under Application of Weak Magnetic Fields

F. A. R. Navarro and Karina L. D. Barturen H.
Universidad Nacional de Educación – Lima, Peru

Abstract

We introduce a proposal for explaining manganites behavior, in the $\text{Pr}_{1-x}\text{Ca}_x\text{MnO}_3$ series with $x=0.30-0.50$. We carry out computer simulations for the Oguchi model along with the crystal field contribution. We contrast the outcomings to experimental measurements made with a commercial magnetometer SQUID. For analyzing the magnetization drop at low temperatures, we take into account quasi-probability distributions.

Key words: Manganites, crystal field; spin Hamiltonians, quantum statistical mechanics.

PACs: 73.22.-f, 75.10.Dg, 05.30.-d

1. Introduction

Manganese oxides, more known as manganites, are magnetic materials with strong electron correlation. Nowadays, there are a great interest of the scientific community in studying it due possible technological applications that may have as in the spintronics and the construction of magnetic refrigerators. The complex magnetic phase diagrams intrigue scientists. Some review articles about these materials are the references [1, 2]. There is a wide variety of phenomenological models, which seek to explain the various features of those exotic compounds. Albeit, so far, there is not an only model that can include all the properties of these materials, many theories have emerged. Namely, we have the following models: exchange double, polaron effect, phase separation in percolative processes and Griffiths singularity. By contrast, several aspects of manganites are an open problem. In this sense, nonextensive statistical mechanics is an alternative to investigate them. That theory has proven to be a guide in the study of manganese oxides [3, 4].

There are some essential ingredients that a system should meet to using the nonextensive statistical mechanics. These requirements are: a) fractal geometry b) memory or long-range interaction, c) inhomogeneities and d) dissipation. There is evidence that the manganites have all of them. For example, A. Satou and M. Yamanaka showed that the manganites have magnetic clusters with fractal way [5], i.e. a Cantor set. Moreover, M. S. Reis *et al.* determined the entropic index q from collected data

with scanning tunneling microscopy, using as sample $\text{La}_{0.7}\text{Sr}_{0.3}\text{MnO}_3$ [4]. They concluded the parameter q represents the degree of magnetic inhomogeneity. This result agrees with the work of E. G. D. Cohen and C. Beck [6].

2. Experimental Measurements

All the measures were made in the Brazilian Center for Research in Physics, CBPF, located in Rio de Janeiro city. We performed measurements with a commercial SQUID magnetometer (model mPMS2), for the compound $\text{Pr}_{1-x}\text{Ca}_x\text{MnO}_3$ with $x = 0.30-0.50$. However, we only show measurements for $x=0.35$, all the other measures are similar. The Table 1 shows the values of mass, temperature and external magnetic field utilized. To obtain the experimental data, the SQUID, properly programmed, used the process known as Zero Field Cooling ZFC, ie. the SQUID magnetometer, in an automated way, cooled the sample without the presence of external magnetic field. Next, to obtaining experimental data, the magnetometer warm up the sample and applied an external magnetic field. In the magnetization is seen a drop at low temperatures, with concentrations $x = 0.30-0.50$ [7, 8]. In Figure 1, we have the curve of magnetization vs temperature, M vs T , for the $\text{Pr}_{1-x}\text{Ca}_x\text{MnO}_3$ with $x = 0.35$. emu is the magnetic unit that uses the SQUID.

Table 1. Utilized data for the SQUID magnetometer measurements.

$\text{Pr}_{1-x}\text{Ca}_x\text{MnO}_3$	Mass (g)	Temperature	External Magnetic Field (T)
$x=0.35$	0.0046	4-300 K	0-5

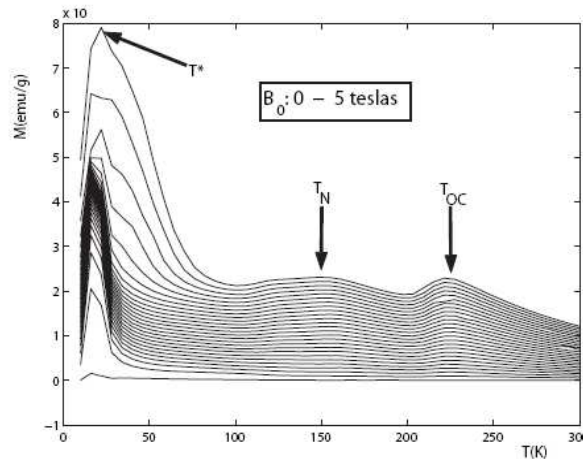


Fig. 1. M vs T experimental curves obtained by a SQUID for $\text{Pr}_{1-x}\text{Ca}_x\text{MnO}_3$, with $x = 0.35$ under application of magnetic fields between 0 T, lower curve, and 5 T, upper curve. Three peaks indicate the critical temperatures of phase transitions.

Before introducing the model based on nonextensive statistical mechanics, we display various interpretations that have this type of graph. For example, V. Hardy *et al.* also

measured it for similar values of x [7]. They interpret there is a metamagnetic transition under application of weak magnetic fields. For doping $x = 0.35$, with external magnetic fields ranging 0-5 T, there are three peaks. The first peak, maximum, is around $T^* = 22$ K. Below it we have a metastable phase, which is ferromagnetic metal. This phase is the product of a first order phase transition from an inhomogeneous phase (ferromagnetic clusters embedded in an antiferromagnetic insulator matrix), after applying the external magnetic field. Measurements with Field Cooling FC procedure show that, in this case, the drop is much less pronounced. According to V. Hardy *et al.* this fact suggests magnetic frustration in this range of low temperatures. The second peak is at $T_N = 149$ K (Neel temperature). Below it, we find a spins ordering, specifically, an antiferromagnetic structure (the works of H. Yoshizawa *et al.* and D. E. Cox *et al.* show that this arrangement is a CE - pseudotype [9]). The third peak is at approximately $T_{OC} = 221$ K. Below it and above T_N there is a charge-order phase. Above T_{OC} we have the paramagnetic insulator phase. When the applied magnetic field is low, 0.2-0.5 T, we observe the disappearance of the antiferromagnetic phase, as well as the elimination of charge-order phase.

In Figure 2 we see the curve of magnetization vs magnetic induction, M vs B . We notice below $T^* = 22$ K the initial slope is constant and determined by the demagnetizing factor. Above this temperature we see a change in the slope. This is a signal of a phase transition, i.e. it passed from ferromagnetic to antiferromagnetic phase. Above $T_N = 149$ K we have the state with charge ordering. And beyond $T_{OC} = 221$ K we observed the paramagnetic state.

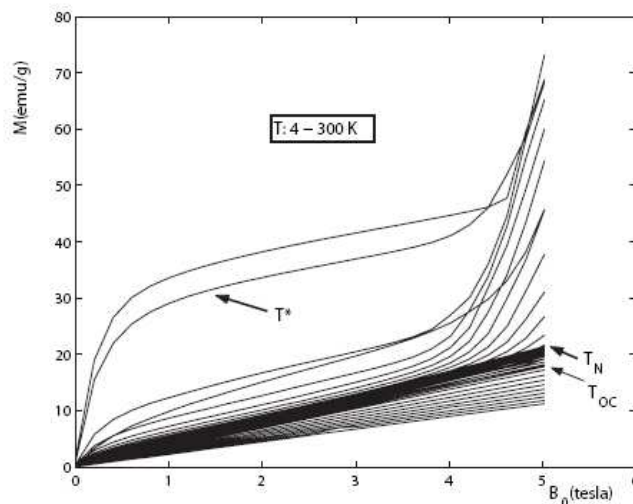


Fig. 2. M vs B_0 experimental curves with the SQUID magnetometer, for the $\text{Pr}_{1-x}\text{Ca}_x\text{MnO}_3$ with $x = 0, 35$. The marked curves correspond to the critical temperatures of phase transitions.

In Figure 3 we show ΔS_m vs B_0 . ΔS_m is the magnetic entropy change in a variation of the magnetic field $\Delta B_0 = 5T$. We observe the critical temperatures which confirm the observations made in the graphs of magnetization.

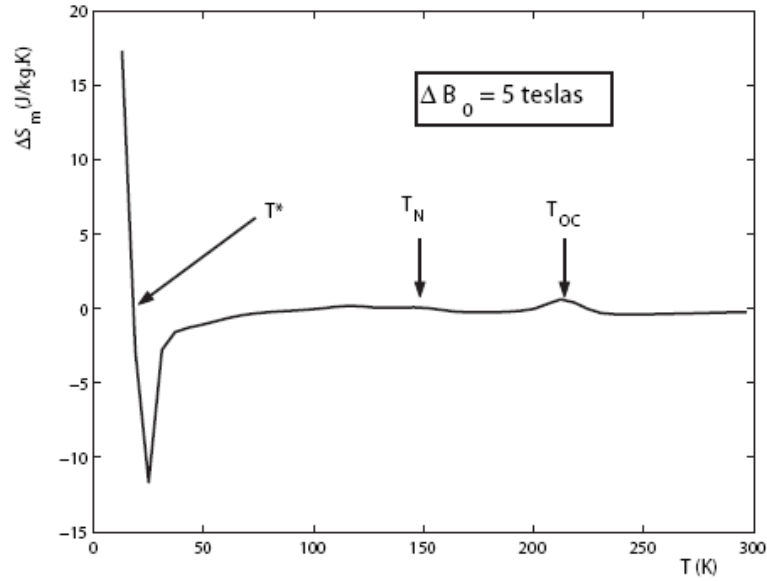


Fig. 3. ΔS_m vs B_0 for the $\text{Pr}_{1-x}\text{Ca}_x\text{MnO}_3$ with $x = 0, 35$. We observe the critical temperatures.

3. Theoretical Frame

In this section we display the tools we will utilize for researching the manganites.

3.1 Nonextensive Statistical Mechanics

On 1988, the Tsallis entropy S_q was postulated as [10]:

$$S_q = k_B \frac{1 - \sum_i p_i^q}{q-1}, \quad (1)$$

where p_i^q is the probability distribution p_i powered to entropic index q , and k_B the Boltzmann's constant, Tr symbolizes the trace operation. Obviously, when q tends to 1, we recover the Boltzmann-Gibbs entropy,

$$S_1 = -k_B \sum_i p_i \text{Ln} p_i. \quad (2)$$

Next, we apply the maximum entropy method to find out what is the minimal probability distribution that maximizes S_q . In this quest we should consider the constraints of unitary norm and internal energy,

$$\sum_i p_i = 1 \quad \text{and} \quad U_q = \frac{\sum_i p_i^q \epsilon_i}{\sum_i p_i^q}, \quad (3)$$

ε_i are the energy eigenvalues. After maximization of S_q , we obtain the following probability distribution p_i :

$$p_i = \begin{cases} \frac{[1 - (1-q)\beta'\varepsilon_i]^{\frac{1}{1-q}}}{Z_q}, & \text{if } 1 - (1-q)\beta'\varepsilon_i \geq 0 \text{ (Tsallis cutoff)} \\ 0, & \text{otherwise} \end{cases} \quad (4)$$

$\beta' = \frac{1}{k_B T}$ is an energy parameter with T the temperature, see the Ref. [11]; Z_q is the partition function,

$$Z_q = \sum_i [1 - (1-q)\beta'\varepsilon_i]^{\frac{1}{1-q}}. \quad (5)$$

The quantum mean values for an observable A , represented by its A_i eigenvalues are given by:

$$\langle A \rangle_q = \sum_i P_i A_i, \quad (6)$$

where we consider the escort distributions:

$$P_i = \frac{p_i^q}{\sum_i p_i^q}, \quad (7)$$

3.2 Quasi-Probability Distributions

The relaxation of Tsallis cutoff Eq. (4) arise negative probabilities. Then, we refer some precedents regarding it. The first distributions of this type were proposed in 1932 by E. Wigner [12]. They arose due impossibility of representing the quantum states of a particle in phase space, and this is a consequence of the Heisenberg's uncertainty principle. On 1948, J. Ville introduced this idea in signal analysis; nowadays is recognized its importance, because those distributions provide a powerful theoretical basis for analyzing in time-frequency. Also, quasi-probability distributions are widely utilized in the study of quantum systems [13], namely, for examining the connections between classical and quantum descriptions. Even more, we have the research of M. O. Scully *et al.* analyzing Feymann's proposal to introducing negative probabilities in order to studying the Young's double slit experiment [14].

3.3 Nonextensive Quasi-Probability Distributions

With evidences that manganites meet the requests for using nonextensive statistical mechanics, we introduce a phenomenological model arising from the proposal to relaxing the Tsallis cutoff. This model will be applied for the magnetization curves with weak magnetic fields, e.g. 0.2 and 0.4 T. The scrutiny of I. G. Deac *et al.* with $\text{Pr}_{0.7}\text{Ca}_{0.3}\text{MnO}_3$ has provided further experimental evidence [8]. Then, we outline the specific mathematical tool to be used. We have relaxation of Tsallis cutoff imply to consider contributions from $1 - (1 - q)\beta'\varepsilon_i < 0$. Therefore, we define the nonextensive quasi-probability distribution as a real quantity:

$$P_i = \text{Re} \left\{ \frac{[1 - (1 - q)\beta'\varepsilon_i]^{\frac{q}{1-q}}}{Z_q} \right\}, \quad (8)$$

the partition function Z_q is defined by:

$$Z_q = \text{Re} \left\{ \sum_i [1 - (1 - q)\beta'\varepsilon_i]^{\frac{q}{1-q}} \right\}, \quad (9)$$

The traditional concept of populations remains to q tending 1 (Boltzmann-Gibbs).

3.4 Model

We take into account the Oguchi model in the mean-field approximation [15], as well as the contribution of the crystal field due to praseodymium. The Oguchi model considers two exactly interacting spins, and the interaction of these spins with a effective field. The crystalline field, caused by electrostatic interactions in the crystal, provokes the removal of the orbital degeneracy t_{2g} and e_g , in the $3d$ ions. So, as a guide for studying $\text{Pr}_{1-x}\text{Ca}_x\text{MnO}_3$ manganites, we use a crystal field of cubic symmetry; more sophisticated models can weigh up a shifting due tetragonal symmetry. For the magnetization, we consider the contribution of magnetic manganese, which has two valences: Mn^{+3} with concentration x , and Mn^{+4} with concentration $1-x$, more the contribution of Pr^{3+} . Thus we have the following Hamiltonian:

$$H_{\text{mag}} = H_{\text{Ogu}} + H_{\text{cc}} \quad (10)$$

where H_{Ogu} is the Oguchi term:

$$H_{\text{Ogu}} = -2\vec{S}_{\text{Mn}^{3+}} \cdot \vec{S}_{\text{Mn}^{4+}} - g\mu_h (S_{\text{Mn}^{3+}}^z + S_{\text{Mn}^{4+}}^z) (B_{\text{Mn}^{3+}} + B_{\text{Mn}^{4+}}), \quad (11)$$

g is the Lande factor, μ_h is the Bohr magneton and $\vec{S}_{Mn^{3+}}$ and $\vec{S}_{Mn^{4+}}$ are the respective spin operators. Also, $B_{Mn^{3+}}$ and $B_{Mn^{4+}}$ are, respectively, the magnetic fields acting on Mn^{3+} and Mn^{4+} :

$$\begin{aligned} B_{Mn^{3+}} &= B_0 + \lambda_{Mn^{3+}} M_{Mn^{3+}} + \lambda_{Mn^{3+}-Mn^{4+}} M_{Mn^{4+}} \quad \text{and} \\ B_{Mn^{4+}} &= B_0 + \lambda_{Mn^{4+}} M_{Mn^{4+}} + \lambda_{Mn^{3+}-Mn^{4+}} M_{Mn^{3+}} \end{aligned} \quad (12)$$

where $\lambda_{Mn^{3+}}$ and $\lambda_{Mn^{4+}}$ are intralattices coupling, $\lambda_{Mn^{3+}-Mn^{4+}}$ stands for the coupling interlattice.

On another side, the H_{cc} term is the contribution of the crystalline field with cubic symmetry of the Pr^{3+} ion. The way of H_{cc} depends on the choice of axes. If we consider the z-axis coinciding with the (100) crystal direction (Miller indices) we have [16]:

$$H_{cc} = W \left\{ \frac{X}{F_4} \right\} (O_4^0 + 5 O_4^4) + \left(\frac{1 - /X/}{F_6} \right) (O_6^0 + 21 O_6^4), \quad (13)$$

where O_4^0 , O_4^4 , O_6^0 and O_6^4 are the Stevens operators for a cubic symmetry [17], they are shown in the Table 2.

Table 2. Stevens operators for a cubic symmetry. J is the quantum number of total angular momentum, J_x , J_y and J_z are components of total angular momentum operator, J_{\pm} are the creation operators (+) and annihilation (-).

$X \equiv J(J+1) \text{ e } J_{\pm} \equiv J_x \pm iJ_y$
$O_4^0 = 35J_z^4 - (30X - 25)J_z^2 + 3X^2 - 6X$
$O_4^4 = \frac{1}{2}(J_+^4 + J_-^4)$
$O_6^0 = 231J_z^6 - (315X - 735)J_z^4 + (105X^2 - 525X + 294)J_z^2 - 5X^3 + 40X^2 - 60X$
$O_6^4 = \frac{1}{4}(11J_z^2 - (X + 38))(J_+^4 + J_-^4) + (J_+^4 + J_-^4)(11J_z^2 - (X + 38))$

Those operators are utilized to quantify the effect of crystal field, that is, the quenching or the attenuation of angular momentum and magnetization.

$$H_{cc} = W \left\{ \frac{X}{F_4} \right\} (O_4^0 + 5 O_4^4) + \left(\frac{1 - /X/}{F_6} \right) (O_6^0 + 21 O_6^4), \quad (14)$$

W , X , F_4 and F_6 are additional parameters, a good reference for them are the calculations carried out by K. R. Lea *et al.* [18].

Then, we aim to showing how the relaxation of Tsallis cutoff leads to a drop in magnetization at low temperatures. So, the Figure 4 shows the experimental curves of magnetization under application of weak magnetic fields, i.e. $B_0 = 0.4$ and 0.2 T. Notice the disappearance of the peaks that mark the antiferromagnetic phase, as well as the charge-order phase; we want stress this behaviour manifests only with weak applied magnetic fields.

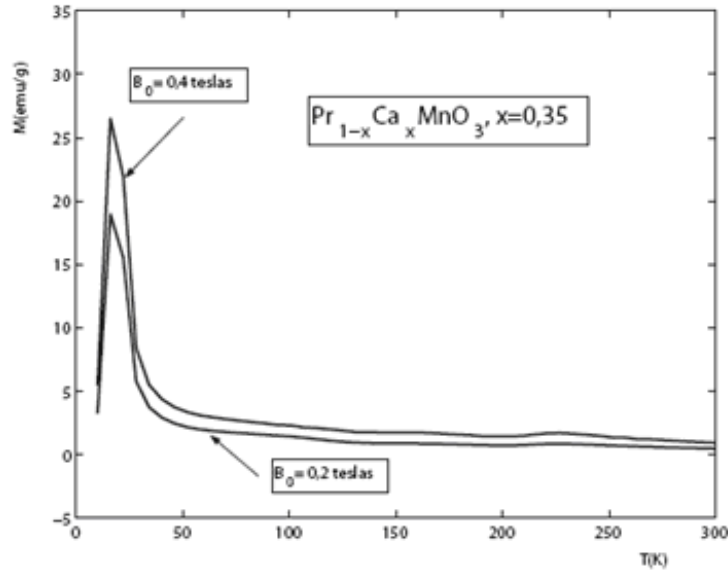


Fig. 4. Experimental curves of M vs T with ZFC, for $\text{Pr}_{0.65}\text{Ca}_{0.35}\text{MnO}_3$ under weak magnetic fields. We observed the disappearance of the antiferromagnetic and charge-order phases, which are evident with magnetic fields greater than 0.2 and 0.4 T, as shown in Figure 1.

The Figure 5 shows the comparison between the experiment and the computational model with nonextensive quasi-probability distributions. Each curve has, respectively, values of magnetic field $B_0 = 0.4$, 0.2 and 0 T.

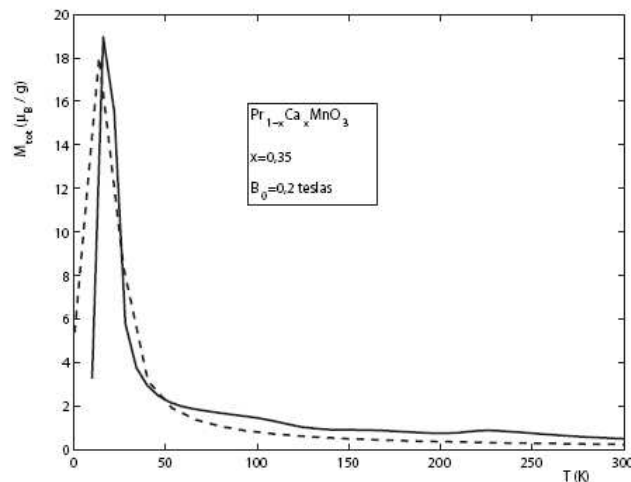


Fig. 5. Solid line: experimental curve for $\text{Pr}_{1-x}\text{Ca}_x\text{MnO}_3$ with $x = 0.35$. Dashed line: computer simulation using the quasi-probabilities. The value of q is 0.55 .

Moreover, we show that this model can also be applied to the experimental curves obtained by I. G. Deac *et al.* [8], with $\text{Pr}_{0.70}\text{Ca}_{0.30}\text{MnO}_3$. In Figure 6 we have an experimental curve of M vs T , under the application of 0.07 T, reproduced from [8].

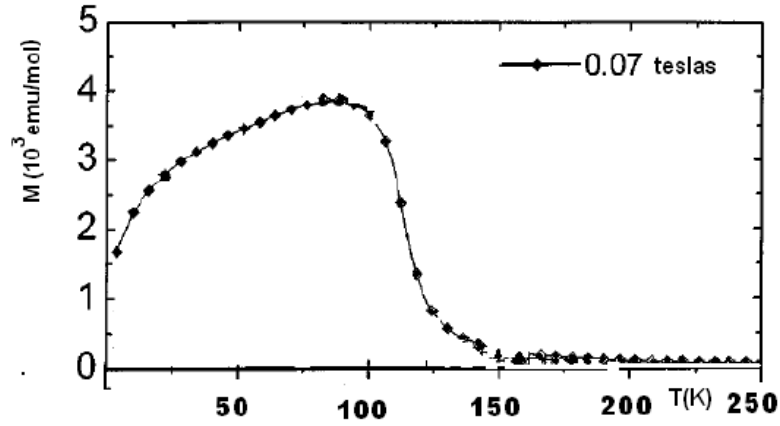


Fig. 6. M vs T measured by I. G. Deac *et al.* [8] for $\text{Pr}_{0.70}\text{Ca}_{0.30}\text{MnO}_3$, using ZFC.

In the Figure 7 we have the graph of M vs T for the same theoretical model from the Figure 5. The former graph suggests, once again, that the relaxation of Tsallis cutoff arise a drop in magnetization at low temperatures for the $\text{Pr}_{0.70}\text{Ca}_{0.30}\text{MnO}_3$. Thus, the new introduced model indicates that the nonextensive statistical mechanics can guide the manganites research.

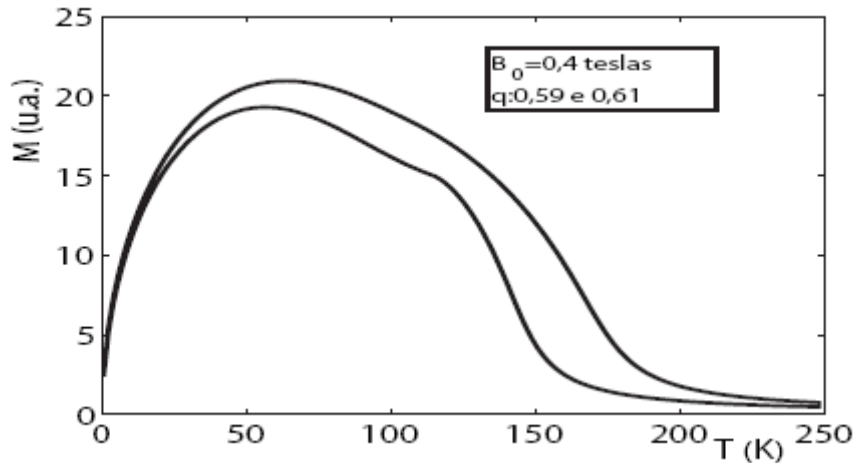


Fig. 7. M vs T for $q = 0.59$ and 0.61 . It is clear the similarity with the Fig. 6.

4. Conclusions

This work displayed a phenomenological model that explains the drop in the magnetization, at low temperatures, for the $\text{Pr}_{1-x}\text{Ca}_x\text{MnO}_3$ series with $x = 0.35$, taking into account low external magnetic fields. The outcomings can be extended for $x=0.35-$

0.50. There were utilized nonextensive quasi-probabilities. These additional probabilities, derived from the relaxation of Tsallis cutoff, cause the drop in the magnetization. The qualitative agreement between the computer simulation and the experimental curves point out, as so much investigations in scientific literature, that the manganites display nonextensive magnetism.

5. Bibliography

[01] E. Dagotto, Science Vol. 309. No. 5732, p. 257 (2005).

E. Dagotto, New J. Phys. 7, 67 (2005).

E. Dagotto, T. Hotta and A. Moreo; Physics Reports 344, No. 1, p. 1 (2001).

E. Dagotto, **Nanoscale Phase Separation and Colossal Magnetoresistance**, Ed. Springer (2008).

[02] Y. Tokura, Rep. Prog. Phys. 69, 797 (2006).

A. M. Haghiri-Gosnet and J. P. Renard; Jour. of Phys. D: Applied Physics 36, Is.8, R127 (2003).

[03] M. S. Reis, J. C. C. Freitas, M. T. D. Orlando, E. K. Lenzi and I. S. Oliveira; Europhys. Lett. **58** (1), 42 (2002).

M. S. Reis, J. P. Araujo and V. S. Amaral, E. K. Lenzi and I. S. Oliveira; Phys. Rev. B **66**, 134417 (2002).

[04] M. S. Reis, V. S. Amaral, J. P. Araujo and I. S. Oliveira; Phys. Rev. B **68**, 014404 (2003).

M. S. Reis, V. S. Amaral, R. S. Sarthour and I. S. Oliveira; Phys. Rev. B **73**, 092401 (2006).

[05] A. Satou and M. Yamanaka; Phys. Rev. B **63**, 212403 (2001).

[06] C. Beck and E. G. D. Cohen; Phys. A **322**, 267 (2003).

C. Beck, Phys. Rev. Lett. 87, 180601 (2001).

[07] V. Hardy, A. Maignan, S. Herbert and C. Martin; Phys. Rev. B 67, 024401 (2003).

V. Hardy, A. Wahl, C. Martin and Ch. Simon; Phys. Rev. B 63, 224403 (2001)

[08] I. G. Deac, J. F. Mitchell and P. Schiffer; Phys. Rev. B 63, 172408 (2001).

[09] H. Yoshizawa, H. Kawano, Y. Tomioka and Y. Tokura; Phys. Rev. B 52, R13, 145 (1995).

[10] C. Tsallis, Phys. D 193, 3 (2004),

C. Tsallis. <<http://tsallis.cat.cbpf.br/biblio.htm>>

G. L. Ferri, S. Martinez and A. Plastino; arXiv:cond-mat/0503441.

[11] C. Tsallis, R.S. Mendes and R. Plastino, Physica A 261, 534 (1998).

[12] E. P. Wigner, Phys. Rev. 40, 749 (1932).

- [13] Liliana Sanz de la Torre, *Aplicacao das Funcoes de Quase-Probabilidade no Estudo da Dinamica de Emaranhamento*, Doctoral Thesis, UNICAMP, SP - Brazil (2003).
- [14] M. O. Scully, H. Walther and W. Schleich; *Phys. Rev. A* **49**, 1562 (1994).
- [15] J. S. Smart, **Effective field theories of magnetism** (Studies in physics and chemistry), Saunders (1966).
- [16] A. P. Guimaraes, **Magnetism and Magnetic Resonance in Solids**, Wiley-Interscience (1998).
- [17] B. Barbara, D. Gignoux and C. Vettier; **Lectures on Modern Magnetism**, Springer-Verlag Berlin (1988).
- [18] K. R. Lea, M. J. M. Leask and W. P. Wolf; *J. Phys. Chem. Solids* **23**, 1381 (1962).